A Series of Highly Ordered, Super-Microporous, Lamellar Silicas Prepared by Nanocasting with Ionic Liquids

Yong Zhou*,† and Markus Antonietti

Max-Planck Institute of Colloids and Interfaces, Research Campus, Golm, D-14424 Potsdam, Germany

Received June 3, 2003. Revised Manuscript Received November 13, 2003

This paper reports a novel preparation of highly ordered monolithic super-microporous lamellar silica with a series of ionic liquids (ILs), 1-alkyl-3-methylimidazolium chloride, as templates via a nanocasting technique. The results show that the silica walls of the formed ordered, super-microporous, lamellar mesostructure were arranged parallel to each other, displaying a very regular structure with ca. 1.2−1.5 nm in pore diameter (in the super-microporous regime), which changed with the chain lengths of the employed templates. Atomic force microscopy and polarized optical microscopy provide direct evidence for the confirmation of the highly ordered and aligned lamellar phase structures of the synthesized monolithic silica. Transmission electron microscopy and low-angle X-ray scattering demonstrate that the ordered, lamellar nanostructure of the prepared super-microporous silica displays no collapse after removal of the template. The formation of potentially two-dimensional crystals of the ILs between the neighboring silica walls by interdigitation of the alkyl chains of the ILs spatially parallel to the imidazole plane is proposed for the templated-formation of the ordered, lamellar super-micropores. The temperature of the sol−gel reaction has been found to have great influences on the molecular spatial aggregates of the ILs, further affecting the pore mesostructure formed.

Introduction

Over the past decade, much effort has been invested to prepare ordered porous materials since the scientists at Mobil Oil Research and Development first synthesized a new family of mesoporous molecular sieves (M41S) with regular, well-defined channel systems by the condensation of aluminosilicate or silicate gels in a concentrated solution of alkyltrimethylammonium ions.[1] The synthesis of the related mesoporous materials relies on a supermolecular templating mechanism, where an assembly of amphiphilic molecules, that is, surfactants, functions as a structure-directing template.[2−5] Such materials of tailored structure and composition show potentials for a wide variety of application in shape-selective catalysts and catalytic supports, low-*k* dielectrics, biomolecular immobilization, molecular separations, solid-phase extraction, or electronic and optoelectronic technologies.[6] Considerable studies have focused on the synthesis of mesoporous materials (pore size > 2 nm) with the aim of increasing pore size by using block copolymer surfactants,[7] or incorporation of swelling agents to synthesis mediums.[8] However, much less attention has been devoted to the synthesis of materials with ordered pores in the super-microporous (pore size 1−2 nm) range.[9−14] The materials in this pore size range are greatly important, since they bridge the gap between microporous zeolites and mesoporous materials. Such materials exhibit the potential of size and shape selectivity for those organic molecules that are too large to access to the pores of zeolithes. Size selective catalysis is hard to be observed in mesoporous materials, because most of the products of catalytic reactions are smaller in size than the mesopores.[15] Although the pore sizes of current templated mesoporous materials, for example M14S, SBA-*n*, HMS, or MSU-X, can be varied during synthesis by choosing

* Corresponding author.
† Current address: Advanced Materials Laboratory, National Institute for Materials Science (NIMS), Namiki 1-1, Tsukuba, Ibaraki 305-0044, Japan. E-mail: zhou.yong@nims.go.jp.

(1) Kresge, C. T.; Leonowicz, M. E.; Roth, W. J.; Vartuli, J. C.; Beck, J. S. *Nature* **1992**, *359*, 710.
(2) Soler-Illia, G. J. D. A.; Sanchez, C.; Lebeau, B.; Patarin, J. *Chem. Rev.* **2002**, *102*, 4093.
(3) Huo, Q.; Margolese, D. I.; Ciesla, U.; Feng, P.; Gier, T. E.; Sieger, P.; Leon, R.; Petroff, P. M.; Schuth, F.; Stucky, G. D. *Nature* **1994**, *368*, 317.
(4) Bagshaw, S. A.; Prouzet, E.; Pinnavaia, T. J. *Science* **1995**, *269*, 1242.
(5) Liu, X.; Tian, B.; Yu, C.; Gao, F.; Xie, S.; Tu, B.; Che, R.; Peng, L.; Zhao, D. *Angew. Chem., Int. Ed.* **2002**, *41*, 3876.
(6) Corna, A. *Chem. Rev.* **1997**, *97*, 2373.
(7) (a) Göltner, C. G.; Antonietti, M. *Adv. Mater.* **1997**, *9*, 431. (b) Göltner, C. G.; Henke S, Weissenberger M. C., Antonietti, M, *Angew. Chem., Int. Ed. Engl.* **1998**, *37*, 613−616.
(8) Beck, J. S.; Vartuli, J. C.; Roth, W. J.; Leonowicz, M. E.; Kresge, C. T.; Schmitt, K. D.; Chu, C. T. W.; Olson, D. H.; Sheppard, E. W.; McCullen, S. B.; Higgins, J. B.; Schlenker, J. L. *J. Am. Chem. Soc.* **1992**, *114*, 10834.
(9) Sun, T.; Wong, M. S.; Ying, J. Y. *Chem. Commun.* **2000**, 2057.
(10) Serrano, D. P.; Aguado, J.; Escola, J. M.; Garagorri, E. *Chem. Commun.* **2000**, 2041.
(11) Bagshaw, S A.; Hayman, A. R. *Chem. Commun.* **2000**, 533.
(12) Zhao, X. S.; Lu, G. Q.; Hu, X. *Chem. Commun.* **1999**, 1391.
(13) (a) Tanev, P. T.; Pinnavaia, T. J. *Science* **1996**, *271*, 1269. (b) Tanev, P. T.; Liang, Y.; Pinnavaia, T. J. *J. Am. Chem. Soc.*, **1997**, *119*, 8616.
(14) McInall, M. D.; Scott, J.; Mercier, L.;Kooyman, P. J. *Chem. Commun.* **2001**, 2282.
(15) (a) Martin, C. R. *Science* **1994**, *266*, 1961. (b) Feng, S.; Bein, T. *Nature* **1994**, *368*, 834.

10.1021/cm034442w CCC: $27.50
Published on Web 12/31/2003

various surfactants with different carbon chain lengths, the smallest pore size that can be obtained appears to be around 2 nm.[12] The synthesis of new types of highly ordered and mechanically stable super-microporous silica still remains a considerable challenge. Most of super-microporous materials reported until now were prepared in the form of micrometer-sized powder, again limiting wider application. To the best of our knowledge, well-defined monolithic super-microporous materials with long-range ordered nanostructure, which have potential for use in continuous separation membrane, sensor, and other nanostructured devices, have not been fabricated yet.[15]

Nanocasting, a versatile method for three-dimensional (3D) transformation of self-assembled organic nanostructures into hollow inorganic replicas with preservation of fine structural details, first introduced by Attard et al.,[16] is a promising tool to come up with such materials. The technique is based on hydrolysis and condensation of inorganic precursors in the aqueous domain of a microphase-separated medium, derived from the self-assembly phase of the template used. As a result, the solidified inorganic compound is thought a replication of the original phase structure, predetermined by selection of the template phase. The size, shape, and connectivity of the formed pore via the nanocasting technique are solely determined by the size and shape of the template that preexists prior to formation of the solid network, rendering significant flexibility for the synthesis of porous materials. The broad potential of nanocasting was just recently reviewed.[17]

Ionic liquids (ILs) are organic salts with low melting points, sometimes as low as −96 °C.[18] ILs have received much attraction in many fields of chemistry and industry, due to their potential as a "green" recyclable alternative to traditional organic solvents.[19] The ILs possess a wide liquidus, in some cases in excess of 400 °C. Their greatly favorable properties, such as negligible vapor pressure, high ionic conductivity, and thermal stability, make the ILs effective in catalysis, electrochemistry, liquid−liquid extraction, and organic liquid-phase reaction. Very recently, IL-based quasi-solid-state electrolytes in combination with an amphiphilic ruthenium polypyridyl photosensitizer were successfully employed for regenerative photoelectrochemical cells that yielded 7% efficiency.[20] Advances in application of the IL/supercritical CO_2 biphasic systems have been recently highlighted,[21] in which the biphasic systems were widely utilized in several catalyzed organic reactions. The first finding of a IL with a melting point of 12 °C was reported in 1914.[22] The most extensively studied ILs are composed of the organic compound 1-alkyl-3-methylimidazolium (abbreviated $[C_n\text{mim}]^+$, where n = number of carbon atoms in a linear alkyl chain). The long-chain ILs have been demonstrated to display the behavior of both lyotropic liquid crystals[23] and thermotropic liquid crystals,[24] which provide a partially ordered environment and a better selectivity for organic reactions.[25]

Recently, we reported initial studies on the preparation of a novel monolithic super-microporous lamellar silica with $[C_{16}\text{mim}]^+Cl^-$, denoted here as $\mathbf{1}_{16}$, as the template employed with the nanocasting technique.[26] The chemical structure of $\mathbf{1}_{16}$ is shown schematically below. The results show that the walls of the perfect, super-microporous, lamellar silica, with an interlayer distance of about 2.7 nm, ca. 1.3 nm in pore diameter, and 1.4 nm in thickness, were arranged parallel to each other, displaying a very regular structure. The present paper describes the preparation of monolithic, super-microporous, lamellar silica with ionic liquids of different carbon chain lengths (designated as $\mathbf{1}_n$). It was found that the produced lamellar pore width varied slightly with the carbon chain lengths of the employed ionic liquids in the range of 1.2−1.5 nm. Atomic force microscopy (AFM) and polarized optical microscopy (POM) provide direct evidence for confirmation of the highly ordered and aligned lamellar phase structure of the synthesized monolithic silica, eliminating the possible misinterpretation as a hexagonal or cubic phase depicted from some specific orientations. The formation of potentially two-dimensional crystals of the ILs between the neighboring silica walls by the interdigitation of the alkyl chains of the ILs spatially parallel to the imidazole plane is proposed for the templated formation of the ordered, lamellar super-micropores. The sol−gel reaction temperature was revealed to have great influence on the mesostructure of the ionic liquid, and further affecting the corresponding templated porous materials to a large extend.

Experimental Section

Preparation of $\mathbf{1}_n$ (n = 10, 14, 16, 18). All the chemicals used in the present work were purchased from Aldrich and used as received. The synthetic procedures of $\mathbf{1}_n$ followed a reported route.[18] As a typical synthesis of $\mathbf{1}_{16}$, 1-hexadecyl chloride (65.24 g, 0.25 mol) was mixed with 1-methylimidazole (20.54 g, 0.25 mol). The mixture was put into a 200-mL flask, refluxed at 90 °C for 24 h, and then cooled to room temperature. A white waxy solid was obtained. The product was dispersed into 200 mL of tetrahydrofuran (THF), from which $\mathbf{1}_{16}$ recrystallized. After washing several times with THF, the crystalline $\mathbf{1}_{16}$ powder was collected by centrifugation and dried in a vacuum at room temperature. The preparation of the other $\mathbf{1}_n$ was achieved by repeating the above procedure with substitution of the corresponding 1-alkyl chloride for 1-hexadecyl chloride, i.e., 1-decyl chloride for $\mathbf{1}_{10}$, 1-tetradecyl chloride for $\mathbf{1}_{14}$, 1-octadecylcholoride for $\mathbf{1}_{18}$.

Preparation of the Monolithic, Ordered, Super-Microporous, Lamellar Silica with $\mathbf{1}_n$ as Templates. In a typical synthesis with $\mathbf{1}_{16}$ as template, tetramethyl orthosilicate (TMOS) was used as the sol−gel precursor. Compound $\mathbf{1}_{16}$ (0.36 g, 1.05 mmol) was mixed with 1.0 mL of TMOS under mild magnetic stirring. After homogenization of the mixture,

(16) Attard, G. S.; Glyde, J. C.; Göltner, C. G. *Nature* **1995**, *378*, 366.
(17) Polarz, S.; Antonietti, M. *Chem. Commun.* **2002**, 2593.
(18) Seddon, K. R.; Stark, A.; Torres, M. J. *Pure Appl. Chem.* **2000**, *72*, 2275.
(19) Welton, T. *Chem. Rev.* **1999**, *99*, 2071.
(20) Wang, P.; Zakeeruddin, S. M.; Comte, P.; Exnar, I.; Gratzel, M. *J. Am. Chem. Soc.* **2003**, *125*, 1166.
(21) Dzyuba, S. V.; Bartsch, R. A. *Angew Chem. Int. Ed.* **2003**, *42*, 148.
(22) Sugden, S.; Wilkins, H. *J. Chem. Soc.* **1929**, 1291.
(23) Bleasdale, T. A.; Tiddy, G. J. T.; Wyn-Jones, E. *J. Phys. Chem.* **1991**, *95*, 5385.
(24) Neve, F.; Francescangeli, O.; Crispini, A. *Inorg. Chim. Acta* **2002**, *338*, 51.
(25) Lee, C. K.; Huang, H. W.; Lin, I. J. B. *Chem. Commun.* **2000**, 1911.
(26) Zhou, Y.; Antonietti, M. *Adv. Mater.* **2003**, *15*, 1452.

0.5 mL of an aqueous solution of 0.01 M HCl as an acid catalyst was added dropwise. The resulting mixture was stirred at 40 °C for 30 min, allowing precondensation of the silica, followed by mild vacuum exposure at 40 °C for removal of the formed methanol due to the hydrolysis of TMOS. Complete gelation was accomplished by leaving the sample in an open flask at 40 °C for 48 h. A transparent, colorless silica monolith was obtained with no visible cracks and very high mechanical stability. The transparency of the hybrid materials strongly suggests the homogeneity of $\mathbf{1}_{16}$ in the silica matrix and the absence of phase separation between the IL and silica. $\mathbf{1}_{16}$ was removed from the silica by calcination of the sample at 550 °C for 3 h with a temperature ramp of 20 °C/min from room temperature to 250 °C and 2 °C/min from 250 to 550 °C. The final product was ground into a powder for further characterization. The other super-microporous silicas were prepared by repeating above procedure with the corresponding as-synthesized $\mathbf{1}_n$ as template.

Characterization. Transmission electron microscopy (TEM) images were acquired on a Zeiss EM 912 Ω at an acceleration voltage of 120 kV. The sample was prepared by applying a drop of a diluted suspension of the silica powder on a carbon-covered copper grid. The phase behavior of $\mathbf{1}_n$ in the reaction medium was studied by polarized optical microscopy (POM) with a Leica DMR optical microscope. Atomic force micrographs (AFM) were collected on the interior of a freshly cleaved monolith. To eliminate the possibility of artificial features being observed in the AFM scan, the images were collected from multiple samples synthesized under the same condition. In all cases, the features observed were entirely reproducible. The low-angle X-ray scattering (LAXS) pattern was recorded on a rotating-anode instrument with pinhole collimation. A Nonius rotating anode device ($P = 4$ kW, Cu Kα) and an image-plate detector system were used. With the image plates placed at a distance of 40 cm from the sample, a scattering vector range from $s = 0.05$ to 1.0 nm^{-1} was available [$s = (2 \sin \theta)/\lambda$, 2θ scattering angle, $\lambda = 0.154$ nm]. Thermogravimateric analysis (TGA) was performed on a Netzsch 209. The sample was examined at a heating rate of 10 °C/min under an oxygen atmosphere. Nitrogen sorption data was obtained with a Micromeritics Tristar 3000 automated gas adsorption analyzer. Before sorption measurements, the samples were degassed in a Micromeritics VacPrep061 degasser overnight at 150 °C under 100 μTorr pressure.

Results and Discussion

Figure 1 shows the TEM images of the resulting pore morphology and structure of the synthesized $\mathbf{1}_n$-templated monolithic silica for (a) $\mathbf{1}_{10}$, (b) $\mathbf{1}_{14}$, (c) $\mathbf{1}_{16}$, and (d) $\mathbf{1}_{18}$. It can been seen that the images b−d display a large domain of a practically ordered lamellar phase, and the pore sizes of the formed lamellar mesostructure increase slightly from 1.2 to 1.5 nm (i.e. in the super-microporous size regime) when the number of the carbon chain atoms of the IL changes from 14 to 16 to 18 under comparable reaction condition, indicating that the long tails of the molecules are packed in an interdigitated conformation. The silica walls show parallelity to each other, as revealed by the corresponding Fourier diffractogram shown in the bottom left inset of Figure 1c, displaying the typical spot pattern of crystal-like order. The top right inset of Figure 1c shows a magnification of the TEM image, revealing an interlayer distance of the formed lamellar nanostructure with $\mathbf{1}_{16}$ as template of about 2.7 nm, with ca. 1.3 nm thick slit pores and a thickness of the wall system of ca. 1.4 nm. The arrows in the inset indicate some potential pillars or touching undulations between the neighboring lamellar layers, supposed to sustain the layered structure of the porous, lamellar material. Similar pillared, porous, lamellar silica has been synthesized by Pinnavaia et al. with vesicular surfactant assemblies.[13]

The formation of the present ordered, lamellar super-micropores is believed to possibly result from the particular spatial aggregation of the IL molecules. Powder X-ray diffractions have confirmed that the alkyl chains of most ILs prefer to be parallel to the imidazole plane in the crystalline state,[27] and the chains interdigitate each other to induce mesophase formation with a bilayer lamellar arrangement of a repeating layer distance in super-microsize.[24,25] In the present case, the reaction temperature of 40 °C is lower than the melting points (50−80 °C)[28] of the employed $\mathbf{1}_{14}$, $\mathbf{1}_{16}$, and $\mathbf{1}_{18}$. With removal of the solvent and methanol by heating during the sol−gel processing of silica at 40 °C, the ILs are expected to gradually crystallize and probably create a two-dimensional crystal between the neighboring silica walls, which act as well-defined templates for the super-micropores. Compared to the $\mathbf{1}_{14}$,$\mathbf{1}_{16}$,$\mathbf{1}_{18}$-templated, very long range ordered, lamellar structures, the long-range order of the produced $\mathbf{1}_{10}$-templated porous silica is apparently disrupted, as marked with the arrow in Figure 1a. This result is consistent with the phase behavior of $\mathbf{1}_n$, of which the analogues bearing shorter ($n = 2-10$) alkyl chains have been reported to be isotropic liquids to some degree at room temperature,[24,25,27] not displaying the perfect interdigitated lamellar arrangement of the 2D-crystalline species.

As to be expected from the mechanism proposed, the sol−gel reaction temperature influences the porous IL-templated mesostructure greatly. Figure 2 presents the TEM image of $\mathbf{1}_{16}$-templated porous silica prepared at the sol−gel reaction temperature of 90 °C, i.e., above the melting point of the ionic liquid. It is clear that the formed pore displays a typical wormlike morphology and is very different from the lamellar phase synthesized at 40 °C. The corresponding average density functional theory (DFT)[29] pore size and the BET surface area of the wormlike porous structure is approximately 2.7 nm and 1316 m^2/g, respectively. The similar wormlike porous structure has been widely prepared with amphiphilic block copolymers (ABCs).[29] The change of the resulting mesostructures at the different sol−gel reaction temperatures is believed to be due to the crystalline/liquid crystalline transition of the ionic liquid. To confirm the phase transition, polarized light optical microscopy (POM) was employed at different temperatures in the present reaction system of $\mathbf{1}_{16}$. Figure 3 shows the POM images of the mesophases of $\mathbf{1}_{16}$ between crossed polarizers of the reaction mixture at 40 °C (a) and 90 °C (b). Very clearly, at 40 °C a "oily streak" texture is found, typical for the lamellar smectic mesophase,[30] confirming that $\mathbf{1}_{16}$ indeed forms a layer-like nanostructure under the applied reaction conditions. At the elevated temperature of 90 °C, a fanlike texture was formed, which is typical for a cylindrical nematic/disordered hexagonal mesophases. The POM experiments therefore confirm the TEM observations.

(27) Holbrey, J. D.; Seddon, K. R. *J. Chem. Soc., Dalton Trans.* **1999**, 2133.
(28) Bowlas, C. J.; Bruce, D. W.; Seddon, K. R. *Chem. Commun.* **1996**, 1625.
(29) Smarsly, B.; Polarz, S.; Antonietti, M. *J. Phys. Chem. B* **2001**, *105*, 10473.
(30) Gray, G. W.; Goodby, J. W. *Smectic Liquid Crystals, Textures and Structures:* Leonard Hill: Glasgow, 1984.

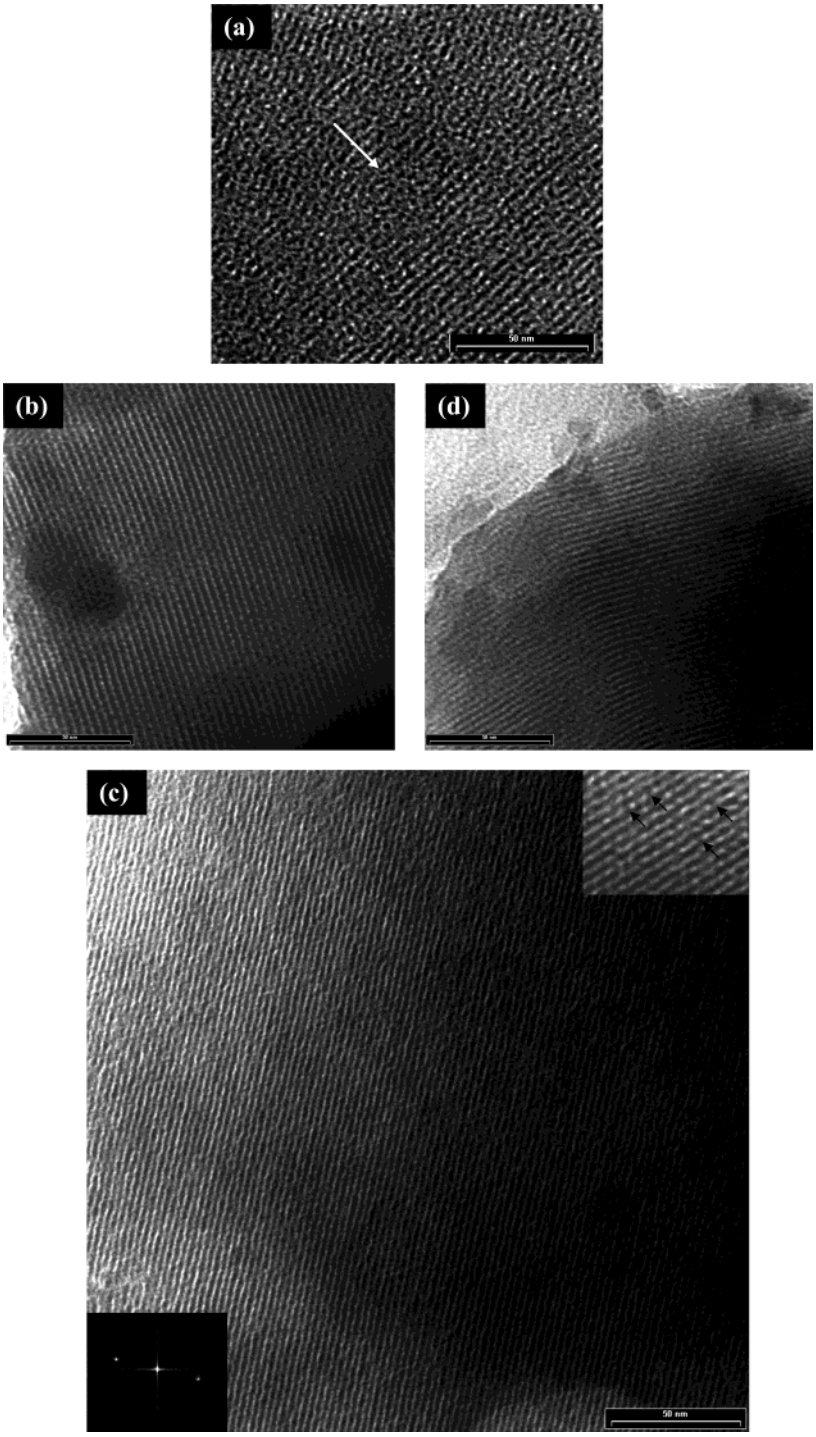

Figure 1. TEM images of the resulting pore morphology and structure of the synthesized $\mathbf{1}_n$-templated monolithic, super-microporous, lamellar silica with the nanocasting technique at the sol−gel temperature of 40 °C for (a) $\mathbf{1}_{10}$, (b) $\mathbf{1}_{14}$, (c) $\mathbf{1}_{16}$, and (d) for $\mathbf{1}_{18}$. The scale bars are 50 nm. Insets in part c are the 1.5× magnification of the image (top right) and the corresponding Fourier diffractogram of the whole picture (bottom left).

AFM was utilized to provide direct and more detailed information on the lamellar structure of the resulting super-microporous silica. Figure 4 shows a typical (a) and the corresponding high-resolution (b) AFM images of the prepared super-microporous silica with $\mathbf{1}_{16}$ as template. As indicated with arrows in Figure 4a, several parallel-stacked sheets of the layer structure can easily be seen. There are no other fracture motives, such a regular pattern of spherical pores, on the surface of the sheet. It means that the layer mesostructure observed in the TEM image in Figure 1 truly originates from a lamellar phase, not from an appropriately fractured hexagonal or cubic phase with some specific orientations. The high-resolution AFM image in Figure 4b reveals more clearly the large-scaled continuous upright orientation of the lamellar phase, as arrow-marked on the corner of the picture. A similar AFM lamellar observation of tin sulfide has been reported by Ozin et al.[31] The fact that the system fractures always perpendicular to the lamellae and not in a slatelike fashion

(31) Sokolov, I.; Jiang, T.; Ozin, G. A. *Adv. Mater.* **1998**, *10*, 942.

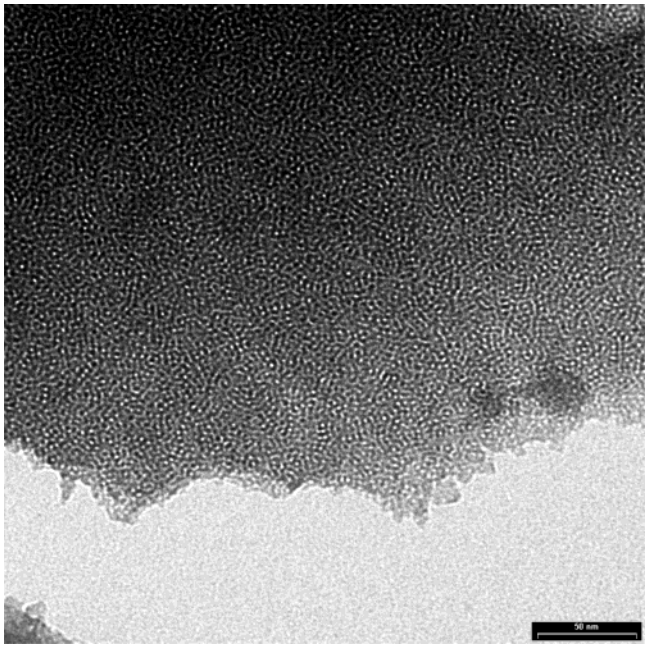

Figure 2. TEM image of $\mathbf{1}_{16}$-templated porous silica prepared at the sol−gel reaction temperature of 90 °C. The scale bar is 50 nm.

shows that the silica nanoplates have regular mechanical weakness (such as perforations or undulations) leading to this extremely homogeneous fracture.

The lamellar mesostructures of the samples were further characterized with low-angle X-ray scattering (LAXS). Parts a and b of Figure 5 show the LAXS patterns of the $\mathbf{1}_{16}$ (a) and $\mathbf{1}_{10}$ (b) templated porous silica, respectively. It is clear that the $\mathbf{1}_{16}$-templated porous silica (a) exhibits a distinct diffraction peak at $2\theta = 3.07°$ with the corresponding d spacing about 2.8 nm, which can be attributed to the (001) reflections of the lamellar framework, in good agreement with the TEM observation. The absence of additional well-expressed (00l) reflections of the lamellar phase may be attributed to structure factor effects. It should be emphasized that the diffraction peak of the as-synthesized $\mathbf{1}_{16}$ silica was found to be slightly too broad according to simple expectations based on the microscopy figures. Compared to short-range ordering of the structure-inducing broadening of the diffraction peaks in our previous wormlike mesoporous systems with block polymers as templates,[17] the most possible reason for the present peak broadening is that the walls of the lamellae are considerably rough or undulating, as already indicated by the TEM image and the fracture behavior of the sample by the AFM image. A comparable broadening of peaks due to undulations is regularly found for self-assembly structures.[32] It is also pointed out that a regular packing of undulations remarkably stiffens even soft matter structures,[33] as seen macroscopically in cardboard or corrugated iron. A similar feature of the LAXS pattern was also observed for the $\mathbf{1}_{14}$- and $\mathbf{1}_{18}$-templated materials. The broadening of the diffraction peak and comparable lamellar pore sizes among $\mathbf{1}_{14}$-, $\mathbf{1}_{16}$-, and $\mathbf{1}_{18}$-templated

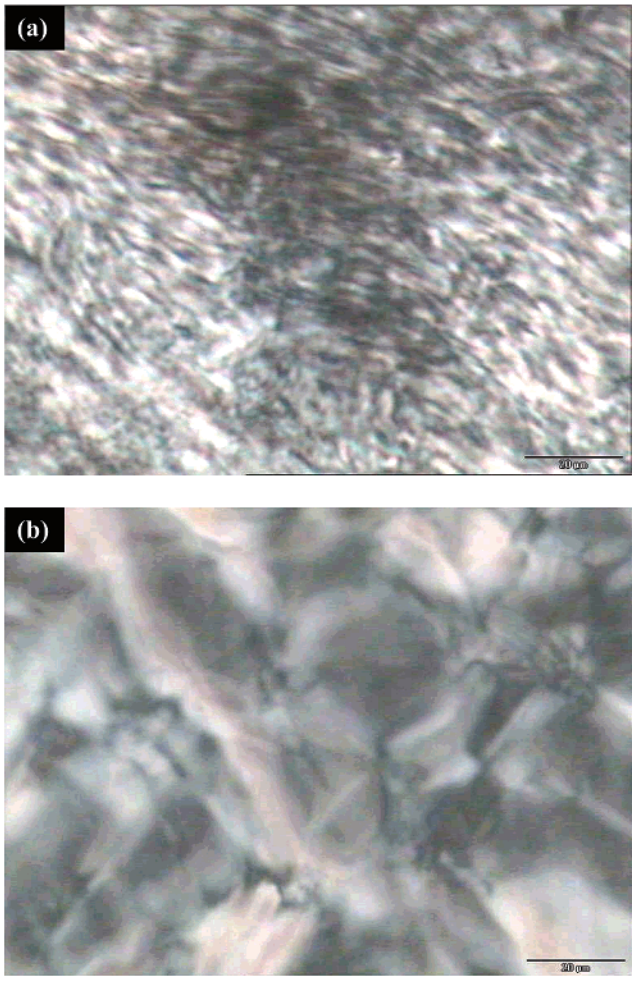

Figure 3. POM images of the mesophase of $\mathbf{1}_{16}$ between crossed polarizers in TMOS, water, and HCl with concentrations as applied at the sol−gel reaction temperature of 40 °C (a) and 90 °C (b) after removal of the solvent and methanol. The scale bars are 20 μm.

materials result in undistinguishing diffraction peak locations among three samples. The $\mathbf{1}_{10}$-templated porous silica (b) exhibits a diffraction peak at 3.09°, which may be assigned to the partially lamellar structure, and the corresponding d spacing is about 2.7 nm. Nevertheless, the obvious decrease in intensity of the diffraction peak in part b compared to that in part a reveals that there is significantly less order of the $\mathbf{1}_{10}$-templated porous silica, which is also consistent with the TEM observation.

The lamellar phases of related surfactant-templated mesoporous materials reported in the literature were always found to collapse after removal of the templates, characterized with nearly featureless XRD patterns.[34] In the present case, both TEM and LAXS indicate practically no collapse of the super-microporous silica structure, in good agreement with another set of super-microporous lamellar nanostructures described previously.[13] We believe that in both cases pillars or touching undulations are responsible for keeping the slit pores open. In addition, a postponement of removal of the surfactant during calcination due to an increased ther-

(32) Antonietti, M.; Kaul, A.; Thunemann, A. *Langmuir* **1995**, *11*, 2633.
(33) Antonietti, M.; Wenzel, A.; Thunemann, A. *Langmuir* **1996**, *12*, 2111.
(34) (a) Kruk, M.; Jaroniec, M.; Yang, Y.; Sayari, A. *J. Phys. Chem. B.* **2000**, *104*, 1581. (b) Kruk, M.; Jaroniec, M.; Yang, Y.; Pena, M. L.; Rey, F. *Chem. Mater.* **2002**, *14*, 4434.

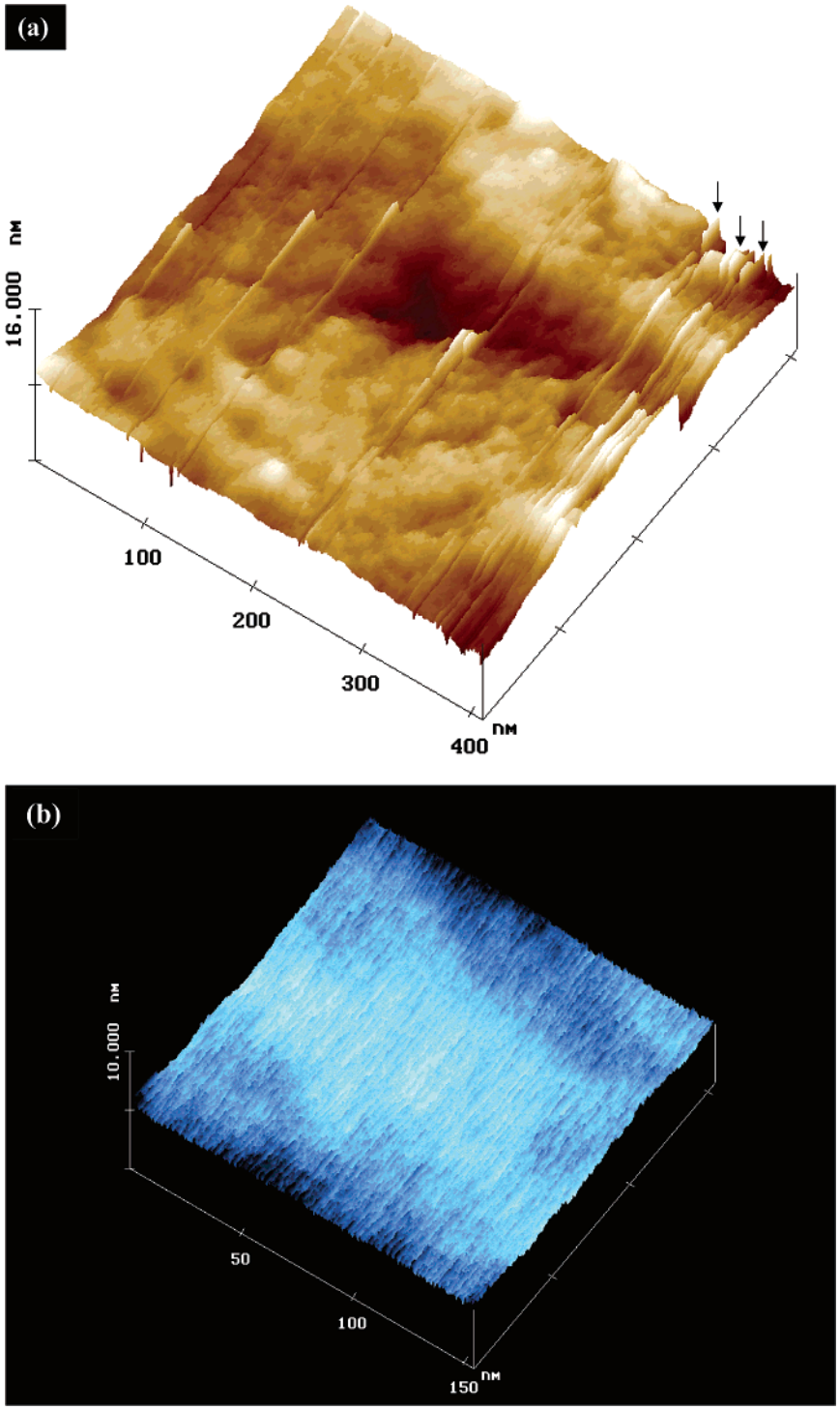

Figure 4. AFM image of the prepared super-microporous silica with $\mathbf{1}_{16}$ as template (a) and the corresponding high-resolution image (b) with the nanocasting technique at the sol−gel temperature of 40 °C.

mal stability in this case will also support the conservation of the lamellar phase, giving the silica framework longer time for the process of condensation and densification at increased temperatures. The higher thermal stability of the IL was tested with TGA on a bare $\mathbf{1}_{16}$ sample in an oxygen atmosphere, and a decomposition temperature of about 287 °C was found, which is 28 and 37 °C higher than those of C_{16}TAB and Pluronics 123, respectively.

Tentatively, the hybrid material was also swelled with organic solvents, expecting to prove the non-interconnected character of the single silica lamellae. The result demonstrates that such a procedure just effectively extracts the IL from the hybrid material, clarifying the weak binding of the template to the wall material and leaving the question of a potential pillaring unanswered.

Figure 6 shows typical N_2 gas adsorption−desorption isotherms of the $\mathbf{1}_{14}$-, $\mathbf{1}_{16}$-, and $\mathbf{1}_{18}$-templated, super-microporous, lamellar silicas made at the sol−gel reaction temperature of 40 °C. It can be seen that all of the isotherms exhibit a transitional type between typical I and IV curves, and no clear presence of hysteresis loops indicates highly uniform pore size and no obvious pore-blocking effect from narrow pores during desorption.[16]

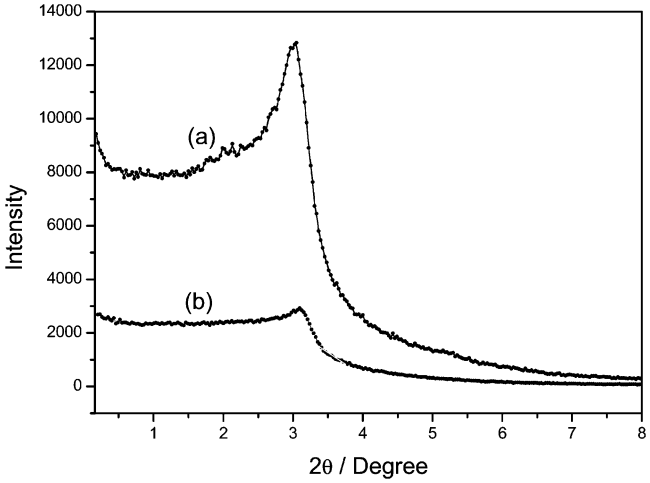

Figure 5. Low-angle X-ray scattering (LAXS) patterns of the synthesized $\mathbf{1}_{16}$ (a) and $\mathbf{1}_{10}$ (b) templated, super-microporous, lamellar silica with the nanocasting technique at the sol−gel temperature of 40 °C.

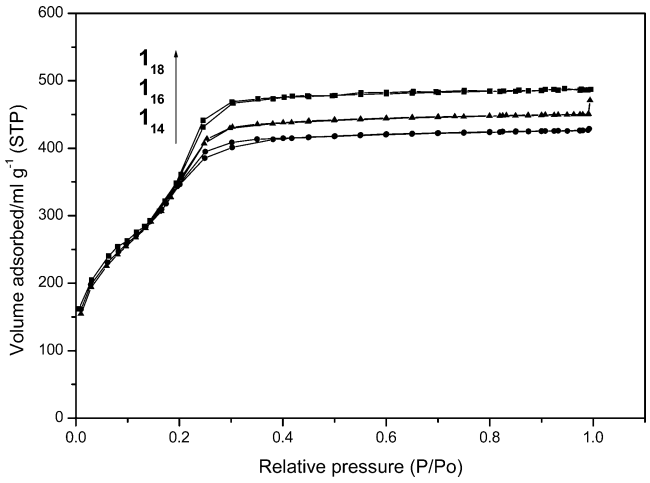

Figure 6. N_2 gas adsorption−desorption isotherms of the synthesized $\mathbf{1}_{14}$-, $\mathbf{1}_{16}$-, and $\mathbf{1}_{18}$-templated, lamellar silicas with the nanocasting technique at the sol−gel temperature of 40 °C.

The isothermal curves also show a pronounced uptake of nitrogen, which occurs clearly at higher relative pressure compared to the previous report of super-microporous silica.[9] We believe that this disparity may result from the variation of morphologies of the super-micropores synthesized, the former ordered lamellar and the latter wormlike, as the behaviors of the sorption isotherms of porous materials are much dependent on not only the pore size but also pore morphology. The present isotherms are actually similar to those published by Kleitz et al.[35] (pore sizes > 2 nm). Furthermore, the adsorption capacities of the present ordered, lamellar, super-microporous silicas, as shown in the isothermal curves, increase with the increasing carbon chains of the ILs at the relative pressure $P/P_o > 0.2$, which is most possibly due to the increase of the lamellar pore sizes, as observed in the TEM images. As expected for the present super-microporous materials, the measured overall BET surface areas of the produced ordered, lamellar, super-microporous silicas with the ILs as template are slightly augmented depending on the carbon chains of the IL used, i.e. 1314 m^2/g for $\mathbf{1}_{14}$, 1340 m^2/g for $\mathbf{1}_{16}$, and 1382 m^2/g for $\mathbf{1}_{18}$ The large surface areas of the samples fit the proposed pore geometry. This also means that "molecular" solvent pores, regularly found not only in xerogels but also omnipresent in standard mesoporous silica,[36] are absent in these special silicas. Here, the material takes a clear profit from the fact that with the ionic liquids a rather big solvent was employed in synthesis, which is not miscible with the silica walls (as opposed to water or oligoethyleneglycols).

Conclusion

In summary, a variety of ionic liquids, 1-alkyl-3-methylimidazolium chlorides, have been used as templates to prepare monolithic, super-microporous silica with lamellar order via the nanocasting technique. The silica walls of the synthesized product were arranged strictly parallel to each other, displaying a very regular structure (ca. 1.2−1.5 nm in pore diameter) with the ionic liquids of different chain length. Atomic force micrographs present a distinguished layerlike structure. Polarized optical microscopy also gives direct evidence for a highly ordered, aligned lamellar phase structure for the synthesized monolithic silica. The transmission electron microscopy and low-angle X-ray scattering prove that the ordered lamellar nanostructure of the prepared super-microporous silica does not collapse after removal of the template. The formation of potentially two-dimensional crystals of the ILs between the neighboring silica walls by the interdigitation of the alkyl chains of the ILs spatially parallel to the imidazole plane is proposed to act as a rather unusual template of the ordered, lamellar super-micropores. Therefore, the sol−gel reaction temperature has important influence on the porous mesostructure. The formed pore at the sol−gel reaction temperature of 90 °C displays a typical wormlike morphology. In addition, the exceptionally high mechanical stability of the material is worth mentioning, indicating the absence of molecular solvent pores, an inherent advantage of using ionic liquids as templates. Further work will be attributed to employ the high robustness of the IL liquid crystals for the generation of other super-microporous materials.

Acknowledgment. Y. Z. appreciates the Alexander von Humboldt (AvH) Foundation for granting a research fellowship. Dr. Jan H. Schattka is thanked for helpful suggestion for the work. Arne Thomas is acknowledged for the TEM measurements.

CM034442W

(35) Kleitz, F.; Blanchard, J.; Zibrowius, B.; Schüth, F.; Agren, P.; Lindén, M. *Langmuir* **2002**, *18*, 4963.

(36) Göltner, C. G.; Smarsly, B.; Berton, B.; Antonietti, M. *Chem. Mater.* **2001**, *13*, 1617.